geoconvention
Virtual Event
September 13 - 15
2021

Full-wavefield applications in migration

Shang Huang and Daniel O. Trad
CREWES, University of Calgary

Summary

Migration of full-wavefield including primary reflections, surface-related multiples, and internal multiples can help with improving the subsurface imaging illumination when the data acquisition geometries are sparse. In this project, we discussed two features using full-wavefield based on the gridpoint response. One is using phase shift plus interpolation to simulate forward modelling wavefields including a multiple generation term. The other feature is to apply a deconvolution imaging condition instead of a cross-correlation imaging condition to update migration results. The outcome shows improved reflection response and amplitude spectrum compared with applying primary wavefield migration. Implementation of using multiple reflection energy can become a complement method for migration.

Theory and Workflow

Full-wavefield applications in migration (Berkhout and Verschuur, 1994; Berkhout, 2014; Verschuur and Berkhout, 2015; Davydenko and Verschuur, 2016; Lu, S., F. Liu, N. Chemingui, A. Valenciano and A. Long, 2018) can become a useful tool to add subsurface information. This project tries to combine multiple energy as the secondary source iteratively in the frequency-wavenumber domain, and uses the deconvolution imaging condition to expand the imaging illumination and accuracy. The workflow is shown in Figure 1.

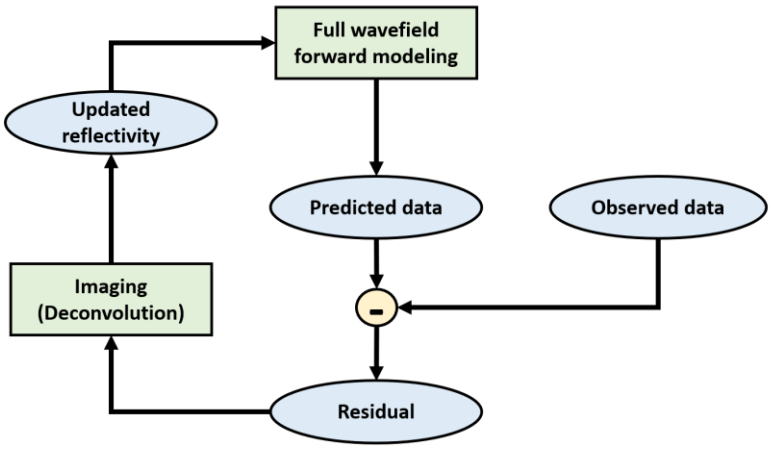

Figure 1: Full-wavefield migration

Forward modeling based on gridpoint response (Berkhout, 2014) can be extended in frequency-wavenumber domain. The downward extrapolated wavefield $\vec{P}^{+}$ at depth z_m can be determined

by the sum of primaries generated by a surface source $\vec{S}^{+}(z_0)$ and scattering wavefields generated by secondary sources or the coda terms at the subsurface $\delta\vec{S}(z_n)$:

$$\vec{P}^{+}(z_m) = \sum_{n<m} \mathbf{W}(z_m, z_n)[\vec{S}^{+}(z_0) + \delta\vec{S}(z_n)], \tag{1}$$

where $\mathbf{W}$ represents extrapolation operators defined by phase shift extrapolation. Then, upgoing wavefields can be obtained by using the scattering wavefields since we assumed no external source at the subsurface:

$$\vec{P}^{-}(z_m) = \sum_{n>m} \mathbf{W}(z_m, z_n)\delta\vec{S}(z_n). \tag{2}$$

For imaging process, we applied *L*2 norm objective function:

$$J = \sum_{\omega}(||\mathbf{P}_{obs} - \mathbf{P}_{mod}||_2^2 + f(\mathbf{R})), \tag{3}$$

where $\mathbf{P}_{obs}$ means the observed data on the surface, $\mathbf{P}_{mod}$ denotes our predicted data. $f(\mathbf{R})$ represents the regularization term, for which we used the Cauchy function criterion (Amundsen, 1991):

$$f\big(\mathbf{R}(z_m)\big) = \frac{1}{2}\sum_{z_m}(1 + \frac{\mathrm{diag}(\mathbf{R}(z_m))^H \mathrm{diag}(\mathbf{R}(z_m))}{\lambda^2}), \tag{4}$$

where $(*)^H$ means the complex conjugate, and the parameter λ corresponds to the scale parameter in the Cauchy distribution. We calculate the gradient of the objective function with respect to the reflectivity coefficient by a deconvolution imaging condition (Valenciano and Biondi, 2003):

$$\mathbf{C}(z_m) = \frac{[\Delta\mathbf{P}^{-}(z_m)][\mathbf{P}^{+}(z_m)]^H}{[\mathbf{P}^{+}(z_m)][\mathbf{P}^{+}(z_m)]^H + \epsilon^2}, \tag{5}$$

which denotes the gradient with respect to the above reflector reflectivity coefficient. $\Delta\mathbf{P}^{-}(z_m)$ represents the back-propagated upward residual, from the data residual on the surface ($\Delta\mathbf{P}^{-}(z_0) = \mathbf{P}_{obs} - \mathbf{P}_{mod}$), and ϵ is a small value for stabilization.

The model update can be determined by:

$$\Delta\mathbf{R}(z_m) = \mathrm{diag}\big(\sum_{\omega}\mathbf{C}(z_m) + f'\big(\mathbf{R}(z_m)\big)\big), \tag{6}$$

where the derivative of Cauchy criterion in terms of reflection coefficient should be

$$f'\big(\mathbf{R}(z_m)\big) = \frac{\mathrm{diag}(\mathbf{R}(z_m))}{1+\lambda^{-2}\mathrm{diag}(\mathbf{R}(z_m))^H \mathrm{diag}(\mathbf{R}(z_m))}. \tag{7}$$

In the next section, some numerical examples will be shown using full wavefields in the migration.

Results

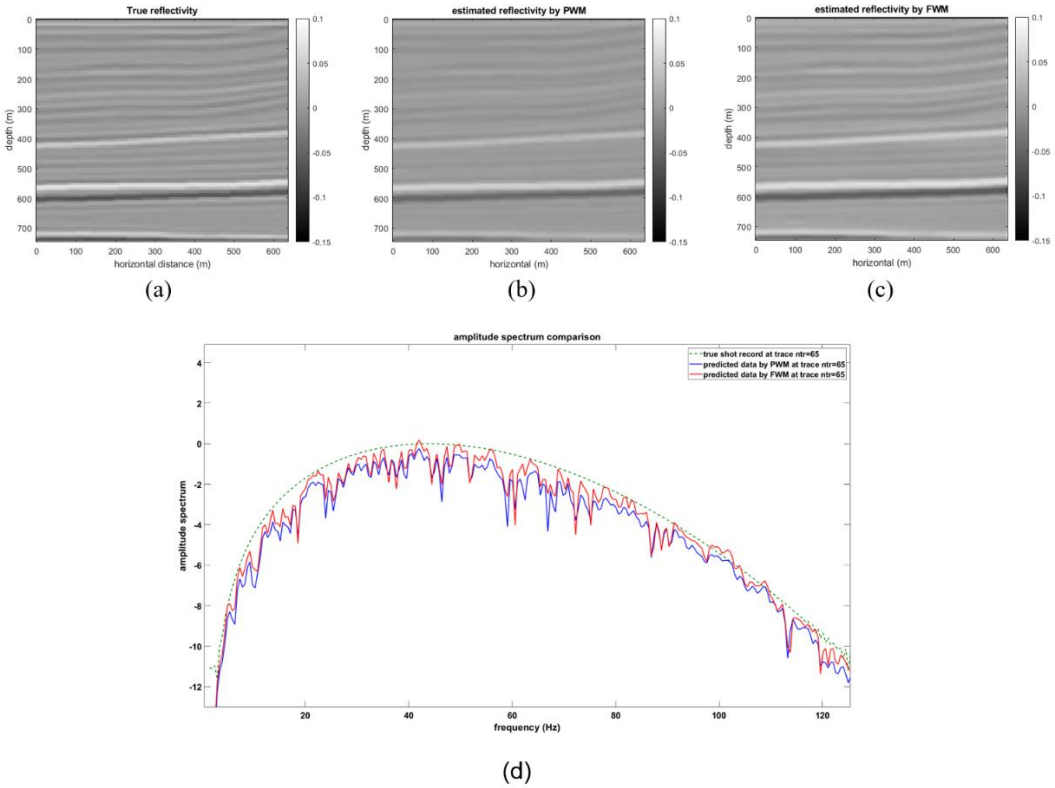

Figure 2. Example for showing the comparison between using full-wavefield and primary wavefield in migration.

For this example, we extracted the left part Marmousi model where Figure 2a is true velocity model. After using full-wavefield in migration, the estimation result had higher reflectivity amplitude (Figure 2c) than the primary wavefield migration (Figure 2b), and full-wavefield migration also can recover some details in the structure. For example, at a depth between 100 to 300 meters and 400 to 550 meters, thin layers' boundaries were clearly estimated by applying full-wavefield energy.

Figure 2d shows a normalized amplitude spectrum comparison at trace 65 between true shot record, primary wavefield modeling and full-wavefield modeling. The high-frequency limitation was around 125 Hz. The full-wavefield result (red line in Figure 2d) had better performance within the bandwidth compared with the PWM result (blue line in Figure 2d). After five iterations, the signal-to-noise ratio of full-wavefield migration was 88.76 %, and that of primary wavefield migration was 73.84 %.

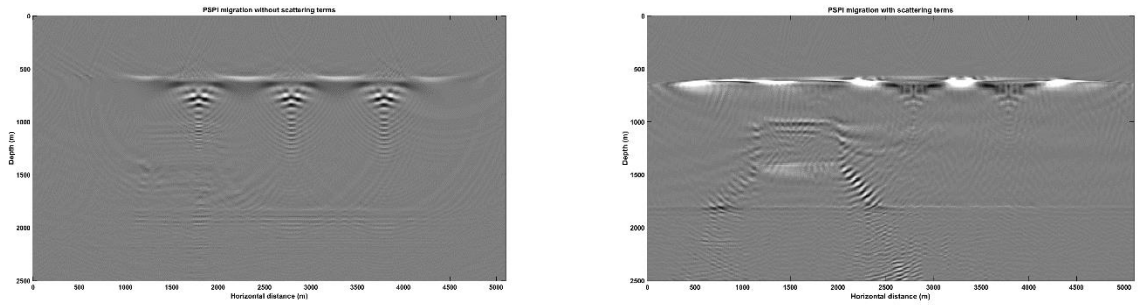

(a) (b)

Figure 3. (a) PSPI migration without scattering terms (b) PSPI migration with scattering terms.

Another model we have tested is the channel model. Figure 3b was the PSPI migration result using scattering terms, which can recover better illumination for the channel structure, provide extended information about deep horizontal event compared with Figure 3a. However, even though implementing multiple reflection energy could help with improving subsurface image illumination and resolution, some unexpected artifacts also show up near the channel. In future work, we will intend to mitigate and remove those artifacts.

Conclusions

This project has examined the uses of full-wavefield in migration compared with applying primary wavefield migration. This algorithm can provide with options to choose different types and orders of reflections we would like to utilize on processing. The results showed that multiple reflection energy is beneficial to expand subsurface structure information compared with primary reflection energy. The deconvolution imaging condition can generate the image with a higher resolution and better lateral continuity compared with applying cross-correlation imaging condition. Additionally, this method can reconstruct the reflectivity coefficients amplitudes in both simple and complicated models. The idea of this approach can become a good start for implementing scattering terms in migration.

Acknowledgements

The authors would like to thank the sponsors of CREWES for continued support. This work was funded by CREWES industrial sponsors, China Scholarship Council (CSC), NSERC (Natural Science and Engineering Research Council of Canada) through the grants CRDPJ 461179-13 and CRDPJ 543578-19. We also thank Dr. Samuel Gray, Dr. Jian Sun, Kristof De Meersman, Xin Fu, Qi Hu and Ziguang Su for valuable discussions, and Dr. Ali Fathalian for his finite-difference modeling code on the MATLAB.

References

Amundsen, L., 1991, Comparison of the least-squares criterion and the cauchy criterion infrequency-wavenumber inversion: Geophysics, **56**, 2027–2035.

Berkhout, A., 2014, An outlook on the future of seismic imaging, part ii: Full-wavefield migration: Geophysical Prospecting, **62**, 931–949.

Berkhout, A., and D. J. Verschuur, 1994, Multiple technology: Part 2, migration of multiple reflections, *in* SEG Technical Program Expanded Abstracts 1994: Society of Exploration Geophysicists, 1497–1500.

Davydenko, M., and D. Verschuur, 2016, Full-wavefield migration: using surface and internal multiples in imaging: Geophysical Prospecting,**65**, 7–21.

Lu, S., F. Liu, N. Chemingui, A. Valenciano and A. Long, 2018, Least-squares full-wavefield migration: The Leading Edge, **37**, 46-51.

Valenciano, A. A., and B. Biondi, 2003, 2-d deconvolution imaging condition for shot-profile migration, *in* SEG Technical Program Expanded Abstracts 2003: Society of Exploration Geophysicists, 1059–1062.

Verschuur, D., and A. Berkhout, 2015, From removing to using multiples in closed-loop imaging: The Leading Edge, **34**, 744–759.